Available online at www.sciencedirect.com
SCIENCE DIRECT®
Polymer 44 (2003) 5381–5386
polymer
www.elsevier.com/locate/polymer

Visualization of block copolymer distribution on a sheared drop

Hyun K. Jeon*, Christopher W. Macosko*

Department of Chemical Engineering and Materials Science, University of Minnesota, Minneapolis, Minnesota 55455, USA

Received 19 February 2002; received in revised form 23 May 2003; accepted 27 May 2003

Abstract

We have visualized a fluorescently-labeled poly(styrene-*b*-methylmethacrylate) (NBD-PS-*b*-PMMA) block copolymer on the surface of a polymethylmethacrylate (PMMA) drop in a polystyrene (PS) matrix. Confocal microscopy revealed that the block copolymer distributed uniformly on the drop surface before deformation. However, in shear flow the copolymer concentration was higher at the tips and edges of the drop. Visualization of drop deformation using a counter-rotating apparatus showed enhanced drop deformation for a drop with block copolymer resulting in larger area generation. Drops with block copolymer showed widening even for shear strains exceeding 10, in contrast to bare drops, which first widened and then shrank. These results agree qualitatively with the observed distribution of fluorescent block copolymer. Copolymer concentration is highest in the regions of high curvature, where lowering interfacial tension should be most effective in retarding drop retraction. Block copolymer on these highly curved surfaces is found to be very effective since the exact theory for zero interfacial tension by Cristini fits our drop widening results well.

Keywords: Block copolymer; Drop deformation; Interfacial tension

1. Introduction

Pre-made and reactively formed block or graft copolymers promote deformation of the minor phase in immiscible polymer blends. Drops elongate further, and in shear flow even widen in the vorticity (x_3) direction, resulting in enhanced generation of area projected onto the velocity–vorticity (x_1-x_3) plane (Fig. 1) [1,2]. This enhanced area is valuable for creating diffusion barrier composites with lamellar microstructure [2].

One explanation for increased drop deformation is that block copolymers lower the overall interfacial tension, Γ, which increases the capillary number, Ca. Ca is defined as the ratio of shear stress to interfacial stress $\eta_m\dot{\gamma}/(\Gamma/R_0)$, where η_m and $\dot{\gamma}$ are the matrix viscosity and the shear rate, respectively, and R_0 is the radius of the undeformed drop. Thus, at constant shear stress, less resistance to drop deformation is expected with lowering interfacial tension. An alternative mechanism is that the deformation creates gradients in the concentration of block copolymer on the drop surface. For the case of surfactants which are insoluble in the bulk phases some numerical simulations have shown that concentration gradients, and thus gradients in interfacial tension, affect drop deformation [3–6]. These simulations have been used to explain experimental observations of sharp drop tips and tip streaming [7–9]. However, there appears to be no direct visualization of surfactant on drop surfaces in the literature. In this paper we report block copolymer distribution at the interface using fluorescently labeled PS-*b*-PMMA (NBD-PS-*b*-PMMA) and show how this distribution appears to influence drop deformation at large shear strain.

2. Experimental

Poly(styrene-*b*-methylmethacrylate) [NBD-PS-*b*-PMMA, M_n = 11K-*b*-23K, M_w/M_n = 1.4] has been labeled with the fluorescent group 7-nitrobenz-2-oxa-1,3-diazole (NBD) [10]. PS (M_n = 105K, M_w/M_n = 1.9) and 1 wt% NBD-PS-*b*-PMMA were blended in solution, precipitated, and dried, and the powder was pressed into 25 mm diameter disks having a thickness of 0.3 mm at 200 °C. PMMA (M_n = 19K, M_w/M_n = 1.8) fibers of 20 to 100 μm diameter were pulled from a molten pellet at 200 °C. Viscosities and

* Corresponding authors. Tel.: +1-612-625-0584; fax: +1-612-626-1686.
E-mail addresses: jeon@cems.umn.edu (H.K. Jeon), macosko@umn.edu (C.W. Macosko).

0032-3861/03/$ - see front matter © 2003 Elsevier Ltd. All rights reserved.
doi:10.1016/S0032-3861(03)00474-9

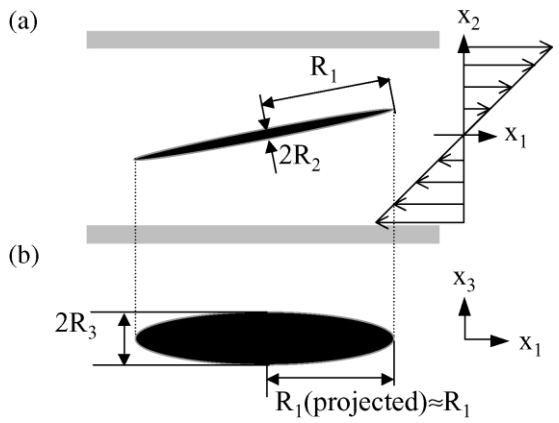

Fig. 1. Schematic of the drop deformation in a counter rotating apparatus: (a) a view in vorticity direction (x_3) and (b) the projection of a drop in x_1-x_3 plane.

storage moduli at 200 °C and $\omega = 1$ rad/s were measured to be 4430 Pa s and 280 Pa and 5790 Pa s and 2010 Pa for PMMA and PS, respectively, with a stress rheometer (DSR, Rheometric Scientific Inc.).

Fig. 2 shows the schematic diagram of the experimental procedure. The fibers were sandwiched between two [PS + 1% NBD-PS-*b*-PMMA] disks followed by annealing at 200 °C for approximately 5 h under N_2 atmosphere. No thermal degradation was observed after annealing. Spherical PMMA drops (PMMA*) were formed by capillary instability of the PMMA fibers. Each drop was covered with a NBD-PS-*b*-PMMA layer as the result of diffusion of NBD-PS-*b*-PMMA in the PS phase to the interface. The sample was quenched using boil off from liquid N_2. The PMMA* drops were removed by dissolving the PS matrix for 3 days using 83/17 v/v cyclohexane/toluene solvent mixture which is a solvent for PS and a nonsolvent for PMMA. The drops were washed 3 times. It was necessary to remove the PMMA* drops, otherwise the large fluorescence from NBD-PS-*b*-PMMA in the PS matrix hides the fluorescent signal from the interface. The PMMA* drops with radii of 20 to 100 μm suspended in a fresh solvent mixture were transferred to the surface of a PS disk (25 mm diameter and 0.5 mm thickness) using a pipet. After drying off the solvent, the PMMA* drops on the PS disk were covered with another PS disk and then heated between 25 mm diameter parallel plates of a rheometer (RMS-800, Rheometric Scientific Inc.) for 30 min at 200 °C. After cooling to room temperature using cold N_2 gas, the sample was removed and the undeformed PMMA* drops in the PS matrix were observed using confocal microscopy (Bio-Rad MRC 1024) with an upright microscope (Olympus AX-70).

The PS disks containing undeformed PMMA* drops were then reloaded in the rheometer at 200 °C, heated for 30 min, and sheared at $\dot{\gamma}_R = 2\ s^{-1}$ for 10 s followed by quenching to temperature below the T_g of PS in less than 10 s. Confocal microscopy observation was repeated on the deformed drops with a strain, γ, less than 10. The NBD-PS-*b*-PMMA was excited with 488 nm wavelength, and the emitted light was filtered to 522 ± 16 nm. A water immersion lens (20 ×, Olympus) was used.

A counter-rotating apparatus [11] was used to visualize drops during deformation in the PS matrix at 200 °C. For the system with NBD-PS-*b*-PMMA, PMMA* drops obtained from the above procedure were embedded between PS disks. The drops without NBD-PS-*b*-PMMA were created directly in the PS matrix by capillary break up of a fiber. In the counter-rotating apparatus we can only view the x_1-x_3 plane thus we measure the projection of R_1 on this plane. Assuming affine deformation the error caused by the projection is 8% at a strain of 2, i.e. the projection of R_1 is 0.92 of the actual value, see Fig. 1. This error decreases with strain [1].

The interfacial tensions for PMMA/PS and PMMA*/PS were measured by the ellipsoid retraction method [12,13]. PMMA and PMMA* drops were sheared to a strain, γ, of 5 followed by the cessation of flow and the shape relaxation measured. Using Taylor's small deformation theory [14] interfacial tension was calculated from the change of drop

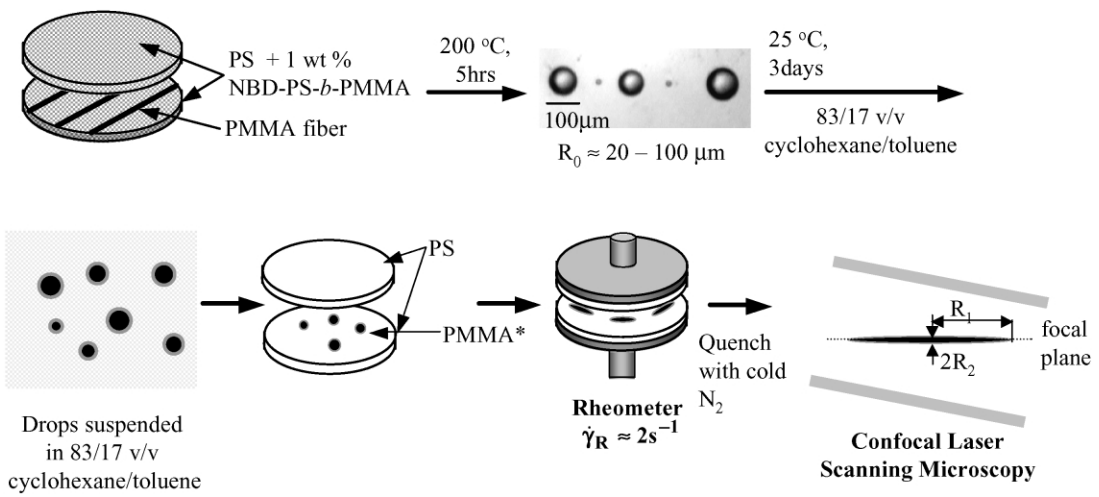

Fig. 2. Schematic of the specimen preparation for confocal microscope observation.

deformation parameter, D, from an ellipsoid to a sphere with time, t.

$$D \equiv \frac{R_1 - R_3}{R_1 + R_3} = D_0 \exp\left\{ -f(\eta_r)\frac{t}{\tau_d} \right\} \quad (1)$$

where,

$$f(\eta_r) = \frac{40(\eta_r + 1)}{(2\eta_r + 3)(19\eta_r + 16)} \quad (2)$$

and,

$$\tau_d = \frac{\eta_m R_0}{\Gamma} \quad (3)$$

D_0 represents the deformation at t_0, R_1 and R_3 are the major and the minor axes of the ellipsoid, respectively, and $\eta_r = \eta_d/\eta_m$. Here, R_1 was calculated from the measured R_3 assuming volume conservation and the axisymmetric ellipsoid, i.e. $R_1 = R_0^3/R_3^2$. For PMMA/PS $\Gamma = 1.9 \pm 0.1$ mN/m, in fair agreement with the literature value (1.5 mN/m at 200 °C [15]). For drops with block copolymer, the interfacial tension is reduced to 1.3 ± 0.1 mN/m.

3. Results

3.1. Undeformed drop and confocal resolution

Fig. 3 shows the confocal microscopy image of a PMMA* drop in the PS matrix before deformation. It is evident from the bright shell that the drop has NBD-PS-*b*-PMMA on its surface. Fig. 3 also shows that the distribution of block copolymer at the interface is uniform before deformation. However, one might expect a very thin layer with the thickness of a block copolymer monolayer, rather than the shell of ~5 μm thickness as seen in Fig. 3. One would also expect to see zero intensity inside the drop. TEM observation revealed that the weak fluorescence inside the drop is not caused by NBD-PS-*b*-PMMA micelles which could be formed by migration of block copolymer from the PS matrix to the PMMA drop [16]. Rather, the increased thickness around the perimeter and the intensity inside the drop originate mainly from spherical aberration of the lens [17].

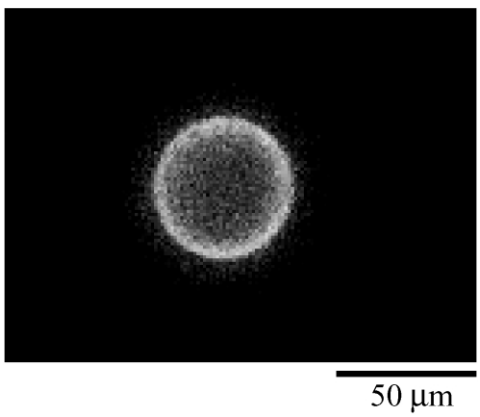

Fig. 3. Confocal microscope image of an undeformed PMMA drop, $R_0 =$ 25 μm, covered with fluorescent NBD-PS-*b*-PMMA layer.

Spherical aberration is caused by the mismatch of refractive indices between the immersion (n_0) and the mount media (n), the numerical aperture, NA, of the lens, and the distance into the specimen (d) [17]. The focal depth difference (δ) caused by the spherical aberration is expressed as:

$$\delta = d\left| \frac{n}{n_0} - \frac{\sqrt{n^2 - NA^2}}{\sqrt{n_0^2 - NA^2}} \right| \quad (4)$$

For our specimen, $d = 500$ μm, $n_0 = 1.33$ (immersion oil), $n = 1.59$ (PS) and NA = 0.5 giving $\delta = 14.8$ μm. Thus the image in Fig. 3 represents the accumulated fluorescence intensity from planes 7.5 μm above and below the focal plane, in this case the equatorial plane.

3.2. Deformed drop and block copolymer distribution

Fig. 4(a) shows the equatorial plane of a drop deformed to a shear strain, γ, of 6 at a shear rate of 0.6 s^{-1}. The drop half thickness, R_2 (see Fig. 2) was estimated to be 6 μm using the pre-deformed drop radius, R_0, 36 μm, fitting the deformed drop image to an ellipse, and assuming constant

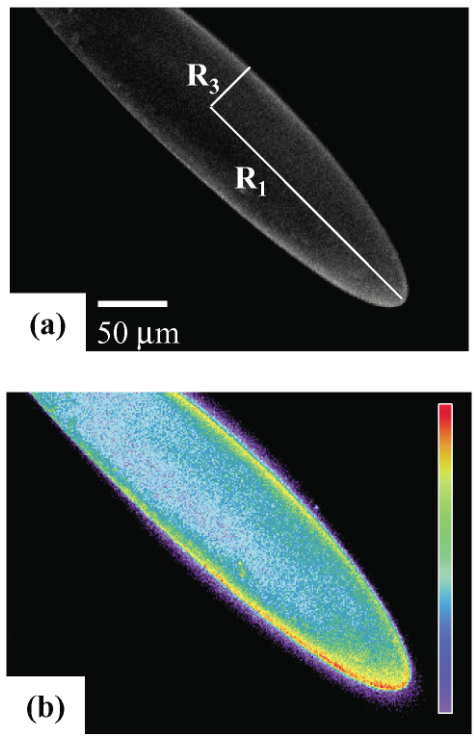

Fig. 4. (a) Confocal microscope image of a PMMA drop, $R_0 = 36$ μm and the half thickness, $R_2 \approx 6$ μm, covered with fluorescent NBD-PS-*b*-PMMA sheared to a strain of 6 in PS matrix at 200 °C followed by quenching to RT. (b) Fluorescence intensity map for (a). After deformation, the tip and the edge show higher intensity, indicating higher concentration of NBD-PS-*b*-PMMA.

volume (see Eq. (5) below). Note that the drop in Fig. 3 was not used to generate the drop in Fig. 4(a). Also note that the drop is so stretched out that its entire thickness is less than half the depth resolution, δ. In addition, the drop surface, except very near the tip and the edge, is so flat that the fluorescence intensity in Fig. 4(a) is very close to representing the block copolymer concentration distribution on the surface. Comparing Figs. 3 and 4(a), the absolute intensity appears to decrease after deformation. This is expected since the surface area increases greatly, and there is no block copolymer inside or outside the drop to diffuse to the new surface. However, the intensity difference between Figs. 3 and 4(a) cannot be compared quantitatively due to quenching of fluorescence groups during annealing before shearing and photobleaching during scanning with the laser light [18].

Fig. 4(b) shows the intensity map for the drop in Fig. 4(a). The intensity map was obtained using MetaMorphII® (Universal Imaging Corp.). In Fig. 4(b), it is clear that the intensity is higher along the drop edge than near the center. Also, the intensity along the edge increases toward the tip. Note that the asymmetric intensity gradient along x_3 direction is due to a slight tilting of the drop when observed. The deformed drop is at an angle between the flow and the deformation directions, thus we manually tilted the drop to align the deformation direction perpendicular to the laser direction to observe the intensity of the equatorial plane (Fig. 2). This manual tilting in x_1 direction caused some tilting in x_3 direction.

3.3. Deformation vs. strain

Fig. 5 shows the deformation vs. strain of a PMMA and a PMMA* drop in the PS matrix. These results are representative of measurements on 4 other pairs of drops. For the drop with the clean surface, Ca is 290 for $R_0 = 90$ μm and the viscosity ratio, $\eta_r = 0.78$. The shear rate was 1.1 s^{-1} determined by fitting R_1/R_0 vs. time at the early stage of deformation, i.e. $2 < R_1/R_0 < 5$. For the drop with block copolymer, $R_0 = 88$ μm, Ca is 340 at $\dot{\gamma} = 0.82$ s^{-1} using $\Gamma = 1.3$ mN/m, and $\eta_r = 0.73$.

Fig. 5(a) and (b) shows the reduced radii R_1/R_0 and R_3/R_0 with strain, respectively. Fig. 5(c) is the plot of projected area ratio A/A_0 defined as the projected area $A = \pi R_1 R_3$ of the deformed drop (assumed to be an ellipsoid) divided by the area of the original drop $A_0 = \pi R_0^2$. The thick straight lines in (a), (b), and (c) are for affine deformation [1,11].

$$
\begin{aligned}
R_1/R_0 &= \left[1 + \gamma^2/2 + \gamma/2(4+\gamma^2)^{1/2}\right]^{1/2} \approx \gamma, \\
R_2/R_0 &= \left[1 + \gamma^2/2 - \gamma/2(4+\gamma^2)^{1/2}\right]^{1/2} \approx 1/\gamma \text{ for } \gamma \\
&\gg 1, \\
R_3/R_0 &= 1
\end{aligned}
\tag{5}
$$

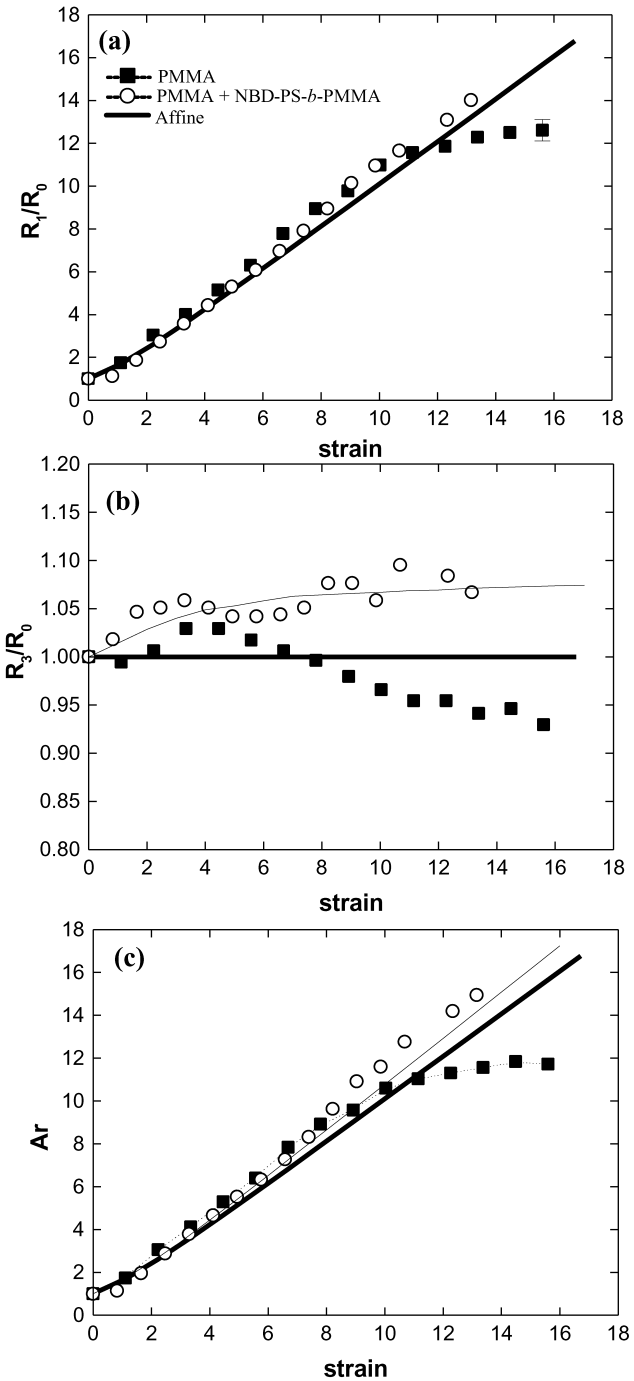

Fig. 5. Reduced radius and reduced area projected onto the flow-vorticity plane plotted as a function of strain for a PMMA drop with and without NBD-PS-*b*-PMMA in PS matrix: Reduced radii (a) in the flow direction R_1/R_0 and (b) the vorticity direction R_3/R_0. (c) Reduced area $A/A_0 = R_1R_3/R_0^2$. For PMMA drop $R_0 = 90$ μm, $\dot{\gamma} = 1.1$ s^{-1}; for PMMA* drop $R_0 = 88$ μm, $\dot{\gamma} = 0.82$ s^{-1}. Solid lines are deformation calculated for zero interfacial tension. Thick lines $\eta_r = 1$ (affine deformation), thin lines $\eta_r = 0.75$ from Cristini [23].

As shown in Fig. 5(a), both drops deform affinely with an error of ±5% up to a strain of 10 above which the PMMA drop nearly stops stretching. However, R_1/R_0 for a PMMA* drop keeps increasing up to the maximum strain we applied,

$\gamma \approx 14$. Beyond this strain the drop became so thin it was difficult to resolve. Following affine deformation up to 10 for the drop without block copolymer is reasonable for the large Ca values used in this study.

In Fig. 5(b), R_3/R_0 for the PMMA drop shows $\sim 3\%$ widening at $\gamma = 4$, and then decreases due to the effect of interfacial tension at the edge with high curvature. R_3/R_0 for the PMMA* drop increases to ~ 1.08 and the widening persists up to $\gamma \approx 14$ resulting in area generation which is greater than affine. For the PMMA drop area generation essentially ceases for $\gamma > 10$ as shown in Fig. 5(c). Note that the experimental error mainly stems from (1) the deviation of a deformed drop from the elliptical shape at strain $> \sim 5$ due to the curvature of this flow between disks, (2) the measurement of drop dimensions using digitized images, and (3) the difficulty in resolving a drop contour at large strains.

4. Discussion

The distribution of the block copolymer on our drops is expected to be dominated by convection. The interfacial Péclet number gives the ratio of convection to diffusion along the interface, $\mathrm{Pe_s} = \dot{\gamma} R_0^2/D_s$. D_s has not been measured but we expect it to be very small, similar to its self diffusion value $\sim 10^{-13}$ cm^2/s for our molecular weight NBD-PS-*b*-PMMA [19,20]. Thus for our drops $\mathrm{Pe_s} > 10^8$. Even at large strains, replacing R_0 with R_2, the radius of curvature near the drop tip, gives $\mathrm{Pe_s} > 10^6$. Thus the local block copolymer concentration is expected to follow the local changes in surface area.

As indicated in Fig. 5(c), at a strain of 6 the drop surface area increases about 6 fold, substantially diluting the block copolymer. However, along the side edge of the ellipsoid area will stay constant, stretching in the x_1-direction proportional to R_1/R_0 but compressing in the x_3-direction proportional to R_2/R_0. At the very tip, area will decrease ideally like $(R_2/R_0)^2$. We see that the concentration distribution of block copolymer in Fig. 4(b) qualitatively matches these area changes. The concentrations on the top and bottom surfaces of the stretched drop are $< 1/3$ of that at the tip, and the edges are slightly lower than the tip. The block copolymer concentration is highest in the regions of high curvature, where lowering interfacial tension should be most effective in retarding the retraction of the drop edges.

Zhou et al. have recently advanced finite element calculations simulations of drop deformation using to three dimensions and to include surfactants [21]. However, these calculations are currently restricted to $\gamma \leq 5$. A useful and readily calculated limit is deformation of a drop with zero interfacial tension. For a drop of viscosity equal to the matrix the deformation is affine and described by Eq. (5). For lower viscosity drops R_1/R_0 will still follow Eq. (5) but a compressive stress develops in the matrix and cause the drop to widen, i.e. $R_3/R_0 > 1$ [22]. Cristini has solved analytically for the drop axes [23]. His results for our viscosity ratio, $\eta_r = 0.75$, are plotted in Fig. 5. The agreement between the exact theory in the limit of zero interfacial tension and the experiment on the drop covered with block copolymer is remarkable and unexpected. By the drop retraction method we only measure a decrease in Γ of 1/3, not nearly enough to give the observed increase in R_3/R_0. The effect of block copolymer gradients on the curved drop surface must be more complex than a simple lowering of the overall interfacial tension.

Surfactant concentration gradients can generate stresses tangent to the interface [5,6], which are known as Marangoni stresses. But these result in a reduction of concentration gradients by acting in the negative x_3 and x_1 directions. The drop retraction experiment used to measure Γ also creates gradients which can cause errors in the measurement [13].

The drop widening observed for the bare PMMA drop in Fig. 5(b) can be compared to boundary integral simulations by Cristini et al. [24]. Current boundary integral methods can reach higher deformations than the 3D finite element method but we still need to extrapolate from the calculated Ca values (20–160) to ours, $\mathrm{Ca} = 290$. This gives $(R_3/R_0)_{max} \approx 1.03$ in good agreement with the experimental results. The maximum area generation before the bare PMMA drop begins to retract occurs at $\gamma \approx 15$. At this strain $R_2/R_0 \sim 1/15$. Substituting this value into the capillary number expression gives the critical capillary number for maximum area generation, $\mathrm{Ca_c} \cong 20$. This value is in good agreement with $\mathrm{Ca_c}$ measured by Levitt and Macosko for several different polymer pairs [1]. Levitt and Macosko postulated that block copolymer might enhance drop deformation by suppressing interfacial slip. Zhao and Macosko have recently measured slip velocity vs. shear stress for PS/PMMA [25]. At the shear stresses generated here, 5000 Pa, they report $v_{slip} < 10^{-2}$ μm/s, which is too low to affect the strain. Moreover, block copolymer concentration decreases linearly with strain on the x_1–x_3 surface, the surface most likely to display slip. Thus at large strain one might expect to see little influence of block copolymer on interfacial slip.

5. Conclusions

Block copolymer distribution on the surface of a polymer drop was visualized using a fluorescently labeled NBD-PS-*b*-PMMA and confocal microscopy. Its effect on drop deformation was observed using a counter rotating apparatus. Before deformation the drop surface had a block copolymer monolayer with uniform concentration distribution. However, shear deformation induced a block copolymer concentration distribution which showed higher concentration at the drop edges and tips. Convection of block copolymer by shear flow is believed to cause the observed distribution; diffusion is not important.

A drop with block copolymer at the interface showed drop widening and stretching into x_3 and x_1 directions, respectively, at $\gamma > 10$. However, for a drop with a clean surface, maximum widening was observed at $\gamma = 4$ followed by retraction, while stretching in the x_1 direction stopped at $\gamma > 10$. For the PMMA/PS interface studied here, the effect of interfacial slip [25] on the deformation is expected to be negligible, and uniform interfacial tension reduction to the value measured by drop retraction, $\sim 2/3$ of that for the bare interface, cannot explain the drop widening. However, Cristini's analysis for zero interfacial tension [23] agrees well with the observed widening. This indicates that the high block copolymer concentration observed along the drop edges must have a strong influence on the interfacial stresses in these regions of high curvature.

Acknowledgements

The authors thank Vittorio Cristini, Sachin Velankar, and Hua Zhou for helpful discussions and comments, and Bongjin Moon for the NBD-PS-*b*-PMMA synthesis. Laura Weatherbee assisted with the experimentation. This work was supported primarily by the MRSEC Program of the National Science Foundation under Award Number DMR-0212302.

References

[1] Levitt L, Macosko CW. Macromolecules 1999;32:6270.
[2] Subramanian PM, Plotzker IG. Barrier materials by blending. In: Paul DR, Bucknall CB, editors. Polymer blends: performance, vol. 2. New York: Wiley; 2000.
[3] Milliken WJ, Stone HA, Leal LG. Phys Fluids A 1993;5:69.
[4] Milliken WJ, Leal LG. J Colloid Interf Sci 1994;166:275.
[5] Pawar Y, Stebe KJ. Phys Fluids 1996;8:1738.
[6] Eggleton CD, Pawar Y, Stebe KJ. J Fluid Mech 1999;385:79.
[7] Hu YT, Pine DJ, Leal LG. Phys Fluids 2000;12:484.
[8] De Bruijn RA. Chem Engng Sci 1993;48:277.
[9] Velankar S, Van Puyvelde P, Mewis J, Moldenaers P. J Rheol 2001; 45:1007.
[10] NBD-PS-*b*-PMMA has been prepared by Dr B. Moon in the Department of Chemistry, U. of Minnesota. First, NBD labeled PS with bromine at the chain end was polymerized by atom transfer radical polymerization (ATRP) using an NBD labeled initiator, 2-[methyl(7-nitro-2,1,3-benzoxadiazol-4-yl)amino]hexyl 2-bromo-propionate. PMMA block was grown from the NBD labeled PS which acted as an ATRP initiator for PMMA polymerization.
[11] Levitt L, Macosko CW, Pearson SD. Polym Engng Sci 1996;36:1647.
[12] Luciani A, Champagne MF, Utracki LA. J Polym Sci 1997;35:1393.
[13] Velankar S, Zhou H, Jeon HK, Macosko CW. Submitted for publication.
[14] Taylor GI. Proc R Soc London 1934;A146:501.
[15] Sundararaj U, Dori Y, Macosko CW. Polymer 1995;36:1957.
[16] Lyu S, Jones TD, Bates FS, Macosko CW. Macromolecules 2002;35: 7845.
[17] Majlof L, Forsgren P-O. Meth Cell Biol 1993;38:79.
[18] Cullander C. Fluorescent probes for confocal microscopy. In: Paddock S, editor. Confocal microscopy methods and protocols. Methods in molecular biology, vol. 22. Totowa, NJ: Humana Press; 1999.
[19] Green PF. Macromolecules 1995;28:2155.
[20] Dalvi MC, Lodge TP. Macromolecules 1993;26:859.
[21] Zhou H, Cristini V, Macosko CW, Lowengrub J. Submitted for publication.
[22] Wetzel ED, Tucker CL. J Fluid Mech 2001;426:199.
[23] Cristini V. Phys Fluids 2002;14:2929.
[24] Cristini V, Hooper RW, Macosko CW, Simeone M, Guido S. Ind Engng Chem Res 2002;41:6305.
[25] Zhao R, Macosko CW. J Rheol 2002;46:145.